High-performance visible-blind GaN-based *p-i-n* photodetectors

Bayram Butun,[a] Turgut Tut, Erkin Ulker, Tolga Yelboga, and Ekmel Ozbay
Nanotechnology Research Center, Department of Physics, and Department of Electrical and Electronics Engineering, Bilkent University, Bilkent, 06800 Ankara, Turkey

(Received 28 November 2007; accepted 21 December 2007; published online 24 January 2008)

We report high performance visible-blind GaN-based *p-i-n* photodetectors grown by metal-organic chemical vapor deposition on *c*-plane sapphire substrates. The dark current of the 200 μm diameter devices was measured to be lower than 20 pA for bias voltages up to 5 V. The breakdown voltages were higher than 120 V. The responsivity of the photodetectors was ~0.23 A/W at 356 nm under 5 V bias. The ultraviolet-visible rejection ratio was 6.7×10^3 for wavelengths longer than 400 nm. © *2008 American Institute of Physics*. [DOI: 10.1063/1.2837645]

The recent developments in high quality GaN/AlGaN material growth technology have led to the realization of high performance solar/visible-blind photodetectors operating in the ultraviolet (UV) spectral region. Some applications in which GaN/AlGaN-based photodetectors are utilized include engine/flame monitoring and detection, plant/vegetation growth monitoring, UV astronomy, and gas detection.[1–6] These photodetectors are also chemically inert and suitable for harsh environments. GaN-based solid-state photodetectors with breakdown voltages of ~100 V,[7–9] responsivities of 0.18 A/W at 360 nm (Ref. 10) (for Schottky type photodetectors) and 0.2 A/W at 355 nm (for back illuminated GaN based *p-i-n* photodetectors) which correspond to 70% quantum efficiency at zero bias,[11] 3 dB bandwidth of 16 GHz (for MSM type photodetectors)[12] and 1.6 GHz (for *p-i-n* type photodetectors)[13] have been previously reported. In this paper, we report our experimental results on high performance GaN photodetectors. Our GaN photodetectors have higher breakdown voltage, lower current density, and higher responsivity when compared to the previously published GaN photodetector results in the literature.

The GaN *p-i-n* structure used in the present study was grown on double-side polished *c*-plane sapphire (Al_2O_3) substrates by low-pressure metal organic chemical vapor deposition (MOCVD) system, which is located at the Bilkent University Nanotechnology Research Center. First, the wafer surface was cleaned by desorption in an H_2 environment at 1080 °C. Then, ~1000 Å AlN nucleation layer was grown at 500 °C by trimethylaluminum (TMAl) and ammonia (NH_3). The wafer surface was recrystallized by annealing at 970 °C. After recrystallization, a high temperature GaN buffer layer of 2500 Å was grown with trimethylgallium (TMGa) and high flow NH_3 at 1160 °C. A *n* layer with a thickness of 5000 Å was grown with silane (SiH_4), in turn, resulting in a carrier concentration of 10^{18} cm^{-3}. The growth continued with a 5000 Å *i* layer. In the last step, an 800 Å *p* layer with Mg doping by biscyclopentadienylmagnesium (Cp_2Mg) was grown.[14,15] In all of the steps, the carrier gas was H_2 and the chamber pressure was kept at 200 mbars.

The samples were fabricated by a six-step microwave-compatible fabrication process[16–18] in class-100 clean room environment. The dry etching was accomplished by reactive ion etching (RIE) under CCl_2F_2 plasma, 20 SCCM (SCCM denotes cubic centimeter per minute at STP) gas flow rate, and 200 W rf power conditions. Mesa structures of the devices were formed via the RIE process by etching all of the layers (>1.2 μm) down to the nucleation layer for mesa isolation. After an Ohmic etch of ~0.74 μm, Ti/Al (100 Å/1000 Å) contacts and Ni/Au (100 Å/1000 Å) contacts were deposited by thermal evaporation and left in acetone for the lift-off process. The Ohmic contacts were annealed at 750 °C for 45 s. Thereafter, a 300 nm thick Si_3N_4 was deposited via plasma enhanced chemical vapor deposition for passivation. Finally, an ~0.4 μm thick Ti/Au interconnect metal was deposited and lifted-off in order to connect the *n*-type and *p*-type Ohmic contact layers to the coplanar waveguide transmission line pads.

For the present study, current-voltage (*IV*), quantum efficiency (QE), capacitance-voltage (*CV*), and high speed measurements were performed. *IV* characterization of the fabricated photodetectors was carried out by using a Keithley 6517A high resistance electrometer with low noise triax cables. QE measurements were performed using a xenon arc lamp, monochromator, UV-enhanced fiber, and SRS lock-in amplifier. The capacitances of diodes were measured by an Agilent 4980A *LCR* meter. The consistency of the measured current levels, in the dark and illuminated cases, was confirmed by all the three current measurement made by these different experimental setups.

The *IV* measurement results in Fig. 1 show that the zero bias dark current of a 200 μm diameter photodetector was

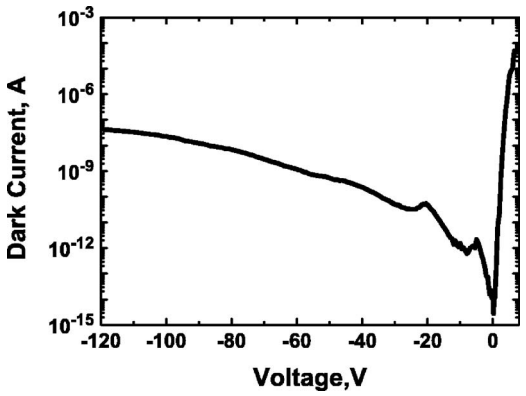

FIG. 1. Current voltage measurements of a photodetector with a 200 μm diameter.

[a]Author to whom correspondence should be addressed. Electronic mail: bbtn@ee.bilkent.edu.tr.

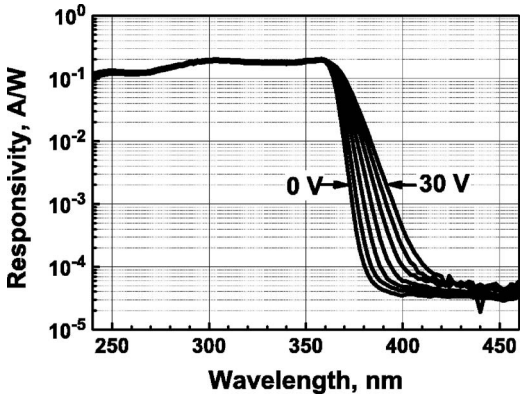

FIG. 2. Responsivity of a 100 μm diameter photodetector for different reverse bias voltages.

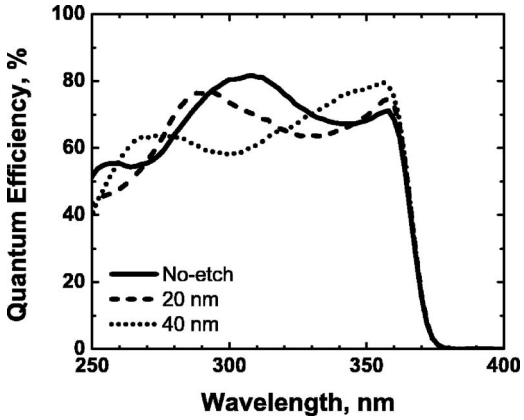

FIG. 4. Spectral quantum efficiency of the photodetector after 0, 20, and 40 nm recess etch of the top dielectric film.

14 fA, and with corresponding current density of 44 pA/cm^2. This current level corresponds to the background noise floor of the electrometer used for the experiments. At 1 V reverse bias, the dark current of the device was 20 fA and at 5 V it was 1.6 pA. The breakdown voltages of the photodetectors were measured to be higher than 120 V.

The turn-on voltage of the fabricated device was around 3 V. The current level of the device for biases below 0.2 V was below the measurement limit. Therefore, a linear fit to the *IV* curve of the device was made for bias values from 0.2 to 0.7 V. Using this linear fit, the ideality factor of the photodiode was calculated as $n=1.97$. The contact resistances were 0.75 kΩ for *n*-type contacts and 15.0 kΩ for *p*-contacts with 100×200 μm^2 contact pads.

We measured responsivity of 100 μm diameter diodes for bias voltages up to 30 V and observed a maximum UV-visible rejection ratio of 6.7×10^3 for wavelengths longer than 400 nm (Fig. 2). Responsivity at 358 nm was 0.20, which corresponds to 70% quantum efficiency. For wavelengths below 360 nm, the responsivity of the devices did not significantly change with applied reverse bias voltages larger than 5 V. Apparently, the diodes were depleted for small voltages, and to confirm this effect we performed *CV* measurements of the fabricated devices.

Figure 3 shows the QE (at 358 nm) and the capacitance measurements of a 100 μm diameter device as a function of applied reverse bias. The QE quickly increased from 64% at 0 V reverse bias to 68% at 5 V reverse bias. For applied reverse biases larger than 5 V, the QE stayed almost constant

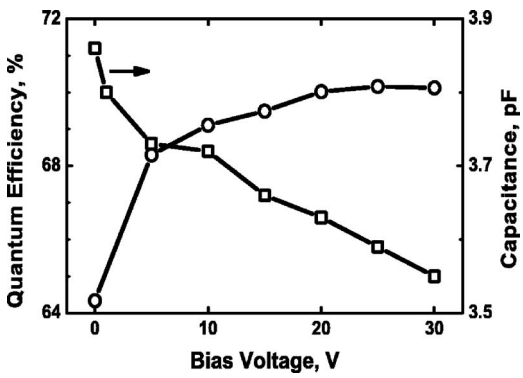

FIG. 3. Voltage dependence of the quantum efficiency and capacitance for 100 μm diode.

with a maximum of 70% at 30 V applied reverse bias. The capacitance of the 100 μm diameter device also had a similar dependency on applied reverse bias. The capacitance quickly dropped from 3.86 pF at 0 V applied reverse bias to 3.7 pF at 5 V applied reverse bias. Afterwards, the capacitance of the device slowly decreased to 3.55 pF as the reverse bias voltage was changed to 30 V. These data clearly showed that most of the intrinsic region was already depleted at very low voltages.

Figure 4 shows that the peak QE of the fabricated device was at 300 nm under 5 V bias. This was in contradiction with the normally expected peak wavelength of 360 nm due to the band gap of GaN. This shift in peak QE wavelength can be explained with the additional optical phase coming from the finite thickness of the deposited dielectric layer. A similar shift was also observed in transfer matrix method (TMM) simulations of the QE for devices with varying top dielectric thicknesses. In order to confirm this explanation by experiments, the top Si_3N_4 layer was etched with diluted $HF:H_2O$ [$\sim3:500$ (ml)] solution in 20 nm. Figure 4 shows the QE measurements after 0, 20, and 40 nm recess etch of the top dielectric film. After a total etch of 40 nm, the peak QE was measured to be 80.1%, while the peak responsivity was 0.23 A/W under 5 V bias at 356 nm. To our knowledge, the 0.23 A/W responsivity value corresponds to the highest responsivity for the front illuminated GaN based *p-i-n* photodetectors reported in the scientific literature.

Using an ultrafast mode-locked fiber laser module with output pulses at 266 nm and 10 ps FWHM (full width at half maximum), we performed the high speed measurement of fabricated *p-i-n* photodiodes. Figure 5 shows the temporal pulse response and the FFT (fast Fourier transform) of the *p-i-n* photodetectors. We measured 48 ps rise time, 351 ps fall time, and 109 ps FWHM from a 100 μm diameter device under 5 V reverse bias voltage. From the FFT data, the corresponding 3 dB bandwidth was found to be 1.16 GHz. This performance is close to the best 3 dB bandwidth of 1.6 GHz reported in the literature for GaN-based *p-i-n* photodetectors.[11]

In conclusion, we report the growth, fabrication, and characterization of high performance GaN-based *p-i-n* photodetectors. The optimized MOCVD growth conditions resulted in epitaxial samples that yielded high performance devices. A maximum 80.1% QE corresponding to 0.23 A/W responsivity at 356 nm, was achieved. The dark current of a

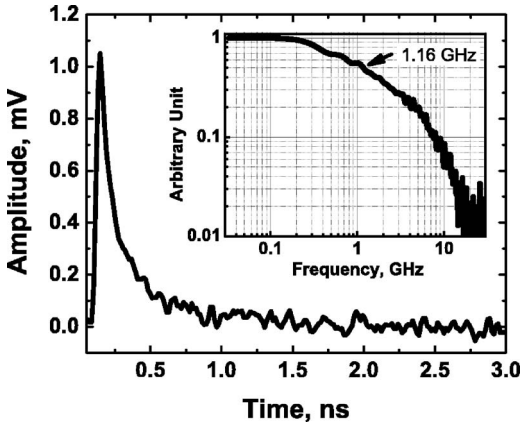

FIG. 5. Temporal pulse response of the 100 μm micron diameter *p-i-n* photodiodes under 5 V reverse bias voltage and the corresponding frequency response (inset).

200 μm diameter circular diodes was measured to be 14 fA, along with a breakdown voltage larger than 120 V. To our knowledge, in terms of breakdown voltage, current density, and responsivity, the reported results are better than the previously published GaN photodetector results in the scientific literature.

This work is supported by the European Union under the projects EU-NoE-METAMORPHOSE, EU-NoE-PHOREMOST, EU-PHOME, EU-ECONAM, and TUBITAK under Projects Nos. 105E066, 105A005, 106E198, 106A017, and 107A012. One of the authors (E.O.) also acknowledges partial support from the Turkish Academy of Sciences.

[1] M. Razeghi and A. Rogalski, J. Appl. Phys. **79**, 7433 (1996).
[2] E. Ozbay, N. Biyikli, I. Kimukin, T. Tut, T. Kartaloglu, and O. Aytur, IEEE J. Quantum Electron. **10**, 742 (2004).
[3] S. J. Pearton, J. C. Zolper, R. J. Shul, and F. Ren, J. Appl. Phys. **86**, 1 (1999).
[4] J. C. Campbell, S. Demiguel, F. Ma, A. Beck, X. Guo, S. Wang, X. Zheng, X. Li, J. D. Beck, M. A. Kinch, A. Huntington, L. A. Coldren, J. Decobert, and N. Tscherptner, IEEE J. Quantum Electron. **10**, 777 (2004).
[5] N. Biyikli, I. Kimukin, T. Tut, O. Aytur, and E. Ozbay, Appl. Phys. Lett. **81**, 3272 (2002).
[6] N. Biyikli, I. Kimukin, O. Aytur, M. Gokkavas, M. S. Unlu, and E. Ozbay, Appl. Phys. Lett. **79**, 2838 (2001).
[7] J. B. Limb, D. Yoo, J. H. Ryou, W. Lee, S. C. Shen, R. D. Dupuis, M. L. Reed, C. J. Collins, M. Wraback, D. Hanser, E. Preble, N. M. Williams, and K. Evans, Appl. Phys. Lett. **89**, 011112 (2006).
[8] B. Yang, T. Li, K. Heng, C. Collins, S. Wang, J. C. Carrano, R. D. Dupuis, J. C. Campbell, M. J. Schurman, and I. T. Ferguson, IEEE J. Quantum Electron. **36**, 1389 (2000).
[9] K. A. McIntosh, R. J. Molnar, L. J. Mahoney, K. M. Molvar, N. Efremov, and S. Verghese, Appl. Phys. Lett. **76**, 3938 (2000).
[10] Q. Chen, J. W. Yang, A. Osinsky, S. Gangopadhyay, B. Lim, M. Z. Anwar, M. Asif Khan, D. Kuksenkov, and H. Temkin, Appl. Phys. Lett. **70**, 2277 (1997).
[11] W. Yang, T. Nohova, S. Krishnankutty, R. Torreano, S. McPherson, and H. Marsh, Appl. Phys. Lett. **73**, 1086 (1998).
[12] J. C. Carrano, T. Li, D. L. Brown, P. A. Grudowski, C. J. Eiting, R. D. Dupuis, and J. C. Campbell, Appl. Phys. Lett. **73**, 2405 (1998).
[13] J. C. Carrano, T. Li, D. L. Brown, P. A. Grudowski, C. J. Eiting, R. D. Dupuis, and J. C. Campbell, Electron. Lett. **34**, 1779 (1998).
[14] H. Yu, M. K. Ozturk, S. Ozcelik, and E. Ozbay, J. Cryst. Growth **293**, 273 (2006).
[15] H. Yu, W. Strupinski, S. Butun, and E. Ozbay, Phys. Status Solidi A **203**, 868 (2006).
[16] N. Biyikli, I. Kimukin, T. Tut, T. Kartaloglu, O. Aytur, and E. Ozbay, Semicond. Sci. Technol. **19**, 1259 (2004).
[17] N. Biyikli, I. Kimukin, O. Aytur, and E. Ozbay, IEEE Photonics Technol. Lett. **16**, 1718 (2004).
[18] B. Butun, N. Biyikli, I. Kimukin, O. Aytur, and E. Ozbay, Appl. Phys. Lett. **84**, 4185 (2004).